Advance and Briefs

Mechanisms of Inactivation of *p14^{ARF}*, *p15^{INK4b}*, and *p16^{INK4a}* Genes in Human Esophageal Squamous Cell Carcinoma[1]

Eric Poe Xing,[2] Yan Nie,[2] Yunlong Song, Guang-Yu Yang, Yuyang Christine Cai, Li-Dong Wang, and Chung S. Yang[3]

Laboratory for Cancer Research, College of Pharmacy, Rutgers, The State University of New Jersey, Piscataway, New Jersey 08854-8020 [E. P. X., Y. N., Y. S., G-Y. Y., Y. C. C., C. S. Y.], and Henan Medical University, Zhengzhou, Henan, 457500 China [L-D. W.]

Abstract

The 9p21 gene cluster, harboring growth suppressive genes *p14^{ARF}*, p15^{INK4b}, and p16^{INK4a}, is one of the major aberration hotspots in human cancers. It was shown that p14^{ARF} and p16^{INK4a} play active roles in the p53 and Rb tumor suppressive pathways, respectively, and p15^{INK4b} is a mediator of the extracellular growth inhibition signals. To elucidate specific targets and aberrations affecting this subchromosomal region, we constructed a detailed alteration map of the 9p21 gene cluster by analyzing homozygous deletion, hypermethylation, and mutation of the *p14^{ARF}*, *p15^{INK4b}*, and *p16^{INK4a}* genes individually in 40 esophageal squamous cell carcinomas (ESCCs) and compared the genetic alterations with mRNA expression in 18 of these samples. We detected aberrant promoter methylation of the *p16^{INK4a}* gene in 16 (40%), of *p14^{ARF}* in 6 (15%), and of *p15^{INK4b}* in 5 (12.5%) tumor samples. Most *p16^{INK4a}* methylations were exclusive, whereas all but one of the *p14^{ARF}*/*p15^{INK4b}* methylations were accompanied by concomitant *p16^{INK4a}* methylation. We detected homozygous deletion of *p16^{INK4a}* in 7 (17.5%), of *p14^{ARF}*-E1β in 13 (33%), and of *p15^{INK4b}* in 16 (40%) tumor samples. Most deletions occurred exclusively on the E1β-*p15^{INK4b}* loci. Two samples contained *p14^{ARF}* deletion but with *p16^{INK4a}* and *p15^{INK4b}* intact. No mutation was detected in the *p14^{ARF}* and *p16^{INK4a}* genes. Comparative RT-PCR showed good concordance between suppressed mRNA expression and genetic alteration for *p15^{INK4b}* and *p16^{INK4a}* genes in the 18 frozen samples, whereas 5 of the 13 cases with suppressed *p14^{ARF}* mRNA expression contained no detectable E1β alteration but aberrations in the *p16^{INK4a}* locus. Our results show that in human ESCCs, *p14^{ARF}* is a primary target of homozygous deletion along with *p15^{INK4b}*, whereas *p16^{INK4a}* is the hotspot of hypermethylation of the 9p21 gene cluster. The frequent inactivation of the *p14^{ARF}* and *p16^{INK4a}* genes may be an important mechanism for the dysfunction of both the Rb and p53 growth regulation pathways during ESCC development.

Introduction

The 9p21 chromosomal band is one of the most frequently altered genomic regions in human cancers (1). Within a short distance of ~50 kb, this region harbors a gene cluster consisting of three genes, *p14^{ARF}*, *p15^{INK4b}*, and *p16^{INK4a}*, all of which have putative tumor suppressor roles (2). In addition to physical proximity, the genomic structures of these genes are remarkably interrelated (Fig. 1). *p14^{ARF}* and *p16^{INK4a}* transcripts are produced via utilization of a common coding sequence for exons 2 and 3, together with distinct sequences for promoter and exon 1 (3). However, the resulting proteins are completely different because different reading frames are used for the respective translation processes (4). The conservation in mammalian genome of this unique gene structure, usually seen in primitive organisms subject to genome size constrains, suggests either the possible ancient origin or the biological essentialness of the unitary inheritance of these two genes. *p15^{INK4b}* is highly homologous to *p16^{INK4a}*, particularly in exon 2, where they share 91% sequence identity (5), indicating their origination by a gene duplication event. The 9p21 gene cluster is the first of its kind identified in the human genome associated with multiple tumor suppressor activities. Besides its functional importance in regulating cell proliferation, which makes this gene cluster a target of selective inactivation during carcinogenic process, there may be a physical basis underlining its frequent disruption in cancer. It was reported that at least two tightly clustered breakpoints exist within the cluster, the sequence context of which potentially facilitates illegitimate V(D)J recombinase activities (6). Furthermore, the promoter regions of all three genes are highly abundant with CpG islands that are susceptible to hypermethylation (7). It is intriguing why presumably important genes are clustered in such a manner that renders high susceptibility to genetic alterations.

Recent studies have revealed that p14^{ARF} and p16^{INK4a} play active roles in the p53 and Rb growth-control pathways, respectively (Fig. 1; Ref. 8). p16^{INK4a} is a cyclin-dependent kinase inhibitor functioning upstream Rb. It can negatively regulate cell cycle progression by preventing the phosphorylation (inactivation) of Rb during G_1 phase (9). p14^{ARF} restrains cell growth by abrogating Mdm2 inhibition of the p53 activity, and therefore facilitates p53 mediated cell cycle arrest and apoptosis (10). It was demonstrated that oncogenic Ras elicits an anti-tumorigenic response mediated by the up-regulation of both p14^{ARF} and p16^{INK4a}, which in turn activate the tumor suppressors p53 and pRb, respectively (11, 12). Recent study further

Received 4/26/99; revised 8/2/99; accepted 8/2/99.

The costs of publication of this article were defrayed in part by the payment of page charges. This article must therefore be hereby marked *advertisement* in accordance with 18 U.S.C. Section 1734 solely to indicate this fact.

[1] Supported by NIH Grant CA65781, facilities from National Institute of Environmental Health Sciences Center Grant ES 05022, National Cancer Institute Cancer Center Supporting Grant CA 72030, and National Natural Science Foundation of China (39840012).

[2] These authors contributed equally to this study.

[3] To whom requests for reprints should be addressed, at Laboratory for Cancer Research, College of Pharmacy, Rutgers University, Piscataway, NJ 08854-8020. Phone: (732) 445-5360; Fax: (732) 445-0687.

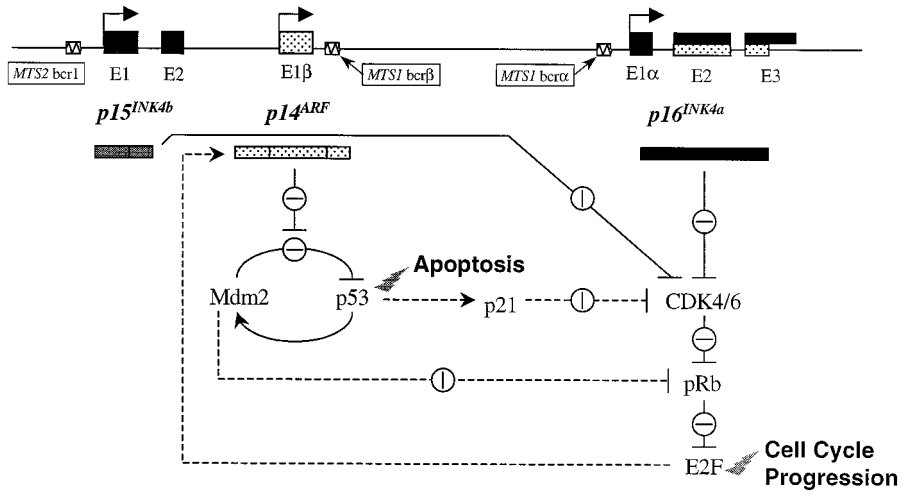

Fig. 1 Genomic organization of the 9p21 gene cluster and schematic description of the involvement of $p14^{ARF}$, $p15^{INK4b}$, and $p16^{INK4a}$ gene products in the pRb and p53 antitumorigenetic pathways [based on a diagram that appeared in Robertson et al. (7)]. *Solid lines*, regulatory steps of each pathway; *dashed lines*, cross-talk between the pRb and p53 pathways.

showed that $p14^{ARF}$ provides a failsafe mechanism for defective Rb pathway by its inducibility via deregulated E2F-1 activity resulted from Rb inactivation (13). Compared with $p14^{ARF}$ and $p16^{INK4a}$, $p15^{INK4b}$ is less prominent as a tumor suppressor. In contrast to $p16^{INK4a}$, which is activated by intracellular stimuli, $p15^{INK4b}$ suppresses cell growth in response to extracellular stimuli such as TGF-β (5).

Inactivation of the Rb and p53 tumor suppressor pathways is observed in most human cancers (1). By virtue of its close involvement in both pathways, the $p14^{ARF}$-$p15^{INK4b}$-$p16^{INK4a}$ gene cluster at chromosome 9p21 may be a nexus of the cellular growth-control network, the inactivation of which results in collapse of the tumor suppression system. To date, a vast amount of data has demonstrated multiple types of genetic alterations on the 9p21 region, the prevalence of which varies with the type of tumors. For example, large homozygous deletions are common in head and neck tumors, bladder carcinomas, and malignant gliomas (14–16). Transcriptional-inactivating promoter methylation was common in breast and colon cancer for the $p16^{INK4a}$ gene (17) and in leukemia for $p15^{INK4b}$ (17, 18). Recently, Robertson *et al.* (7) identified that the promoter of $p14^{ARF}$ gene is a CpG island and observed its hypermethylation in colon cancer cell lines, which was responsible for the gene inactivation (7). Point mutation and small deletion of the $p16^{INK4a}$ locus was common in pancreatic adenocarcinoma, biliary tract cancers, and hereditary melanoma (reviewed in Ref. 19) and affected $p16^{INK4a}$ exclusively or together with $p14^{ARF}$ (4). Despite the ample evidence of the 9p21 gene cluster as a frequent tumor target, it is not known whether all three genes in the cluster are indiscriminately affected in a tumor and whether all of the genes are uniformly disrupted by the same mechanism.

We reported previously an alteration pattern of the 9p21 region in human ESCC,[4] in which $p16^{INK4a}$ was primarily affected by hypermethylation and less frequently subject to deletion, whereas $p15^{INK4b}$ was frequently homozygously deleted and occasionally methylated (20). This pattern is different from reports on other types of cancers identifying $p16^{INK4a}$ as the main deletion target and $p15^{INK4b}$ as a bystander, which possibly play a small part in the tumor suppressor role (2). In light of the recent elucidation of the tumor suppressor role of $p14^{ARF}$, the first exon of which is only 12 kb downstream of the $p15^{INK4b}$ gene, and the presence of evidence of exclusive deletion of $p14^{ARF}$-E1β with the retention of both $p15^{INK4b}$ and $p16^{INK4a}$ in T-cell acute lymphoblastic leukemia (21), we suspect that our previous result may indicate $p14^{ARF}$-E1β as being a primary target for inactivation in ESCCs. In consideration of this point, we thought it is necessary to investigate whether genomic alterations indeed associate with altered gene expressions in ESCCs. In the present study, we constructed a detailed alteration map of the 9p21 gene cluster by analyzing the homozygous deletion and aberrant methylation of the $p14^{ARF}$, $p15^{INK4b}$, and $p16^{INK4a}$ genes individually in 40 resected ESCC samples and analyzed the mRNA expression pattern of the respective genes in 18 frozen samples. We show that suppressed mRNA expression occurred at a high frequency for all three genes in primary ESCCs, and homozygous deletion is the primary cause leading to such inactivation for the $p14^{ARF}$ and $p15^{INK4b}$ genes, whereas aberrant methylation is the main event underlining $p16^{INK4a}$ inactivation.

Materials and Methods

ESCC Specimen Preparation and RNA/DNA Extraction. Eighteen primary ESCC specimens, together with their adjacent normal epithelial tissues, were collected from patients in Linzhou City (formerly Linxian) of northern China, a well-recognized high-risk area for ESCC. The samples were frozen in liquid nitrogen right after surgical resection and were kept in −70°C until processing for RNA/DNA extraction. Adjacent normal epithelia accompanying the tumors were identified through pathological examination and dissected directly from the tissue blocks. All tumor tissues were embedded in OTC and cryosected into 15-μm serial slides under −20°C. H&E staining and histopathological examination were performed on a repre-

[4] The abbreviations used are: ESCC, esophageal squamous cell carcinoma; HD, homozygous deletion; kNN, k-Nearest-Neighbor; GAPDH, glyceraldehyde-3-phosphate dehydrogenase.

Table 1 Summary of oligonucleotides[a]

Primer loci	Analytical purpose	Primer sequence/Genomic site	Product size (bp)
p16^{INK4a} exon 1α	HD	GAGCAGCATGGAGCCTTC AATTCCCCTGCAAACTTCGT	204
p16^{INK4a} exon 2	HD	CACTCTCACCCGACCCGT ACCTTCCGCGGCATCTAT	222
p14^{ARF} E1β 1st half	HD and SSCP	TCCCAGTCTGCAGTTAAGGG TGAACCACGAAAACCCTCAG	177
p14^{ARF} E1β 2nd half	HD and SSCP	GTTTTCGTGGTTCACATCCC CACCAAACAAAACAAGTGCG	178
p15^{INK4b} exon 2	HD	ACCGGTGCATGATGCT TCAGTCCCCCGTGGCTGT	172
p16^{INK4a}	mRNA expression	CAACGCACCGAATAGTTACG AGCACCACCAGCGTGTC	176
p14^{ARF}	mRNA expression	GTTTTCGTGGTTCACATCCC ACCAGCGTGTCCAGGAAG	264
p15^{INK4b}	mRNA expression	GGAATGGGCGAGGAGAACAAGGGCATG ATAAGCTTGGCGTCAGTCCCCCGTGGCT	428
p14^{ARF} E1β	Methylated specific	GT**C**GAGTT**C**GGTTTTGGAGG AAAACCACAAC**G**AC**G**AAC**G**	160
p14^{ARF} E1β	Unmethylated specific	TGAGTTTGGTTTTGGAGGTGG AACCACAACAACAAACACCCCT	165
β-*Actin*	Internal control	CTGTGGCATCCACGAAACTA AGGAAAGACACCCACCTTGA	187
GAPDH	Internal standard	TCTCATGGTTCACACCCATGACGAACATG AAGAAGATGCGGCTGACTGTCGAGCCACAT	456

[a] In methylated- and unmethylated-specific primers, Ts (or As for antisense) that were converted from Cs by bisulfite modification were underlined. Unchanged Cs (or Gs for antisense) were in bold case.

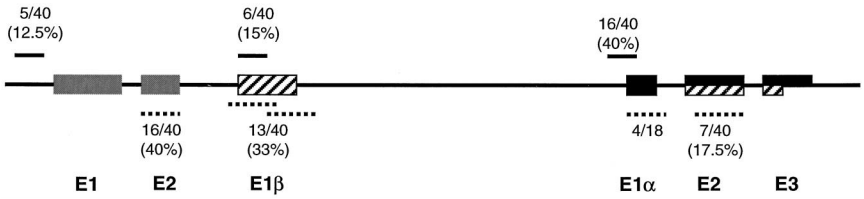

Fig. 2 Genomic positions of the PCR targets. The regions that were amplified and their genomic positions for hypermethylation analysis (*solid lines*) and HD (*dashed lines*) are shown. The alteration numbers and percentages are shown *above* or *below* the *lines*. The sequence of *p14^{ARF}* was taken from GenBank (accession no. L41934). The sequences of *p16^{INK4a}* and *p15^{INK4b}* are as described previously (20).

sentative section from each tissue block to identify the tumor region. Tumor tissues were then dissected from the neighboring three consecutive sections. Polyadenylated RNA was extracted from both the normal and tumor tissues using the Rneasy Mini kit (Qiagen, Santa Clarita, CA) according to the manufacturer's specification. To ensure complete comparability of the analyses at the DNA and RNA levels, all leftover remnants from mRNA preparation were reused for genomic DNA extraction by proteinase K digestion and phenol/chloroform extraction. Another 22 pairs of tumor and normal DNAs from the paraffin-embedded ESCC specimens were directly taken from a sample collection (previously analyzed for *p16^{INK4a}* and *p15^{INK4b}* status; Ref. 20) and were further examined for *p14^{ARF}* molecular alterations. All of the primers used in this study are listed in Table 1.

Methylation-specific PCR and Methylation Status Verification by Sequencing. Aberrant methylation was detected using the CpG WIZ Amplification kit (Oncor, Gaithersburg, MD), following the protocol provided. Except for *p14^{ARF}* gene, for which the primers used in the analysis were designed by ourselves (Table 1 and Fig. 2), primers for *p16^{INK4a}* and *p15^{INK4b}* analysis came with the kit. The DNA was modified by bisulfite reaction and then underwent two separate PCR reactions using unmethylated-specific and methylated-specific amplifiers. The bisulfite treatment converts the unmethylated cytosine to uracil and thus makes the sequence of unmethylated DNA read differently from that of the methylated DNA after modification. Methylation was determined by the presence of methylated-specific PCR products.

To verify the methylation status determined by methylation-specific PCR, products from methylated and unmethylated-specific PCR reactions were cloned using the TOPO TA cloning kit (Invitrogen, Carlsbad, CA). For both types of PCR reactions, five clones were randomly picked up, and the cloned fragments were sequenced directly.

Homozygous Deletion Analysis Using Duplex PCR. HDs of the *p16^{INK4a}*-E1α, E2, *p14^{ARF}*-E1β, and *15^{INK4b}* genes were examined using methods established previously in our laboratory (20). In brief, each gene locus was analyzed by comparative multiplex PCR using the β-actin fragment as internal standard and a closely sized PCR fragment of the gene as

the primary target. About 100 ng of DNA were used for the duplex PCR amplification. Forward primers of both target gene and control were radiolabeled at the 5′ end with [γ-^{33}P]dATP. After 27–29 cycles of PCR, the products were resolved on 6% denaturing or 8% nondenaturing polyacrylamide gel, depending on product size difference. After autoradiograph for 4 h, the film was developed, and the ratio of intensity of the target gene *versus* control was measured and calculated using a computer imaging system (Image-Pro Plus; Media Cybernetics, Silver Spring, MD). A HD was scored if the normalized signal intensity (target/β-actin) in the tumor sample was <25% of that in the normal epithelium. The threshold was so chosen because of an estimated upper limit of 20–25% noncancerous cell contamination in our tumor samples.

Measurement of mRNA Expression of the *p14^{ARF}*, p15^{INK4b}, and *p16^{INK4a}* Genes. cDNA was synthesized using the Advantage RT-for-PCR kit (Clontech, Polo Alto, CA) with random priming as recommended in the protocol provided. Comparative PCRs were performed with the *GAPDH* gene as internal standard and one of the gene in the 9p21 gene cluster as target. PCR cycle numbers (typically 27–30 cycles) were experimentally determined in pilot studies to limit the reaction in the linear stage. PCR products were resolved on 20% nondenaturing polyacrylamide gel or 3% agarose gel, and signal intensities were quantified using a computer image system. The levels of the gene transcripts were quantified by the ratio of the intensity of the target signal over the intensity of the GAPDH internal standard in the same duplex PCR reaction.

Statistical Pattern Recognition and Data Classification. To establish a reasonable criterion discriminating the different mRNA expression states, expression level data measured from all tumor and normal samples for a single gene were subject to automatic pattern recognition and clustering using the standard kNN method (22), where the "k" was set at 3. This procedure was performed independently for each gene of interest. A density-distribution curve was calculated and plotted using S-PLUS statistical package on a Sparc-3 Station, and evaluation of normality of the density distribution was done by comparing the distribution with a normal distribution using "qqnorm" plot done by S-PLUS. kNN classifier was coded in the C programming language and run on a Unix Ultra-Sparc 3 system. Detailed mathematical discussion, program description, and general data experiment of this method will be summarized in a separate report.

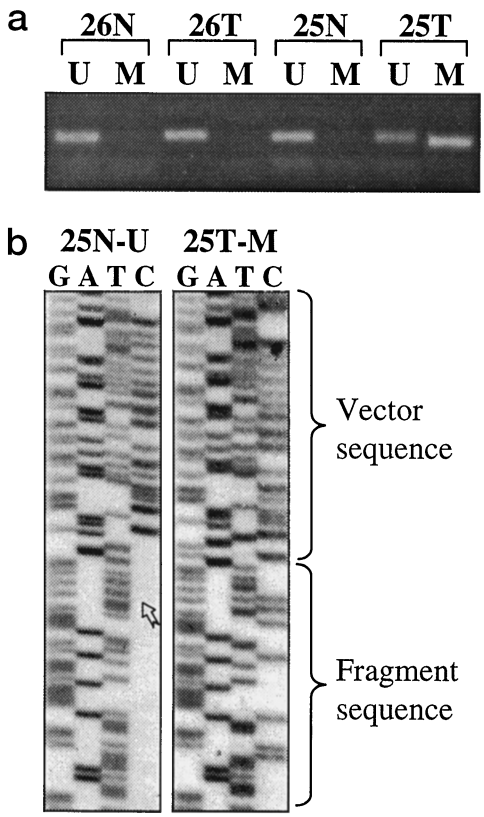

Fig. 3 Determination of the methylation status of the CpG islands (using *p14^{ARF}* analysis as an example). *a*, methylation-specific PCR analysis. Two pairs of samples, representing presence of CpG island hypermethylation in tumor but not in normal DNA (no. 25), or no such event in either tumor or normal DNA (no. 26), are shown as examples. CpG methylation is determined by the presence of PCR product amplified by methylated-specific primers (M). Lack of methylation is evidenced by the presence of only PCR product amplified by unmethylated-specific primers (*U*) but not the methylated-specific product. *b*, confirmation of methylated-specific PCR by sequencing the PCR fragments. In the unmethylated-specific PCR product (*25N-U*, the cloned fragment as marked under the cloning vector), all of the "*C*"s were converted to "*T*"s (*arrow*), but in the methylated-specific product (*25T-M*), the "*C*"s in CpG dinucleotides were unchanged because of methylation, which resisted chemical modification by bisulfite.

Results

Aberrant Methylation of 5′-CpG Islands in 9p21 Gene Cluster. The methylation status of the *p14^{ARF}*, *p15^{INK4b}*, and *p16^{INK4a}* CpG islands were investigated in 40 ESCC samples together with their adjacent normal epithelial tissues. Among them, 18 were frozen samples and 22 were from a collection of paraffin-embedded specimens analyzed previously for *p15^{INK4b}* and *p16^{INK4a}* alterations (20); enough DNA remained for analyses of *p14^{ARF}* alterations. Using methylation-specific PCR (Fig. 3*a*), among the 40 samples, we detected aberrant methylation of the *p14^{ARF}* gene in 6 samples (15%), of the *p15^{INK4b}* gene in 5 samples (12.5%), and of the *p16^{INK4a}* gene in 16 samples (40%). The frequency of the *p15^{INK4b}* and *p16^{INK4a}* methylation is consistent with our previous observation (20). The aberrant methylation of *p14^{ARF}* in primary tumors, to our knowledge, has not been previously reported. Ten of the 16 *p16^{INK4a}*-methylation cases were observed exclusively on the *p16^{INK4a}* promoter region. On the other hand, four of the six cases with *p14^{ARF}* methylation and four of the five cases with *p15^{INK4b}* methylation occurred in samples in which all three genes have aberrant methylation. In many cases, in addition to the presence of methylation-specific PCR signal, a PCR signal corresponding to the unmethylated DNA sequence could also be detected from the same samples. The unmethylated signals might come from stromal cells present between the cancer nests, which could not be completely removed in our microdissection procedure. To verify the specificity of the PCR reaction, we sequenced the PCR products that resulted from both methylated-specific amplifiers and unmethylated-specific amplifiers and

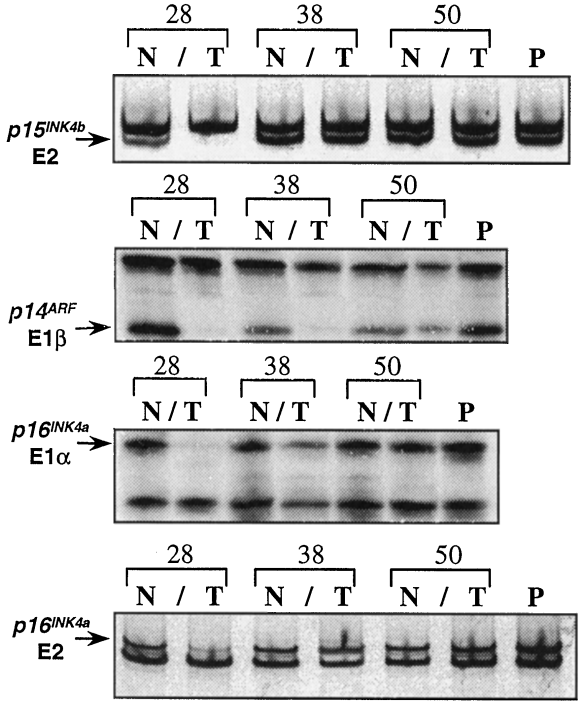

Fig. 4 HD of the $p14^{ARF}$-E1β, $p15^{INK4b}$, and $p16^{INK4a}$-E1α, E2 in primary ESCCs determined by duplex PCR. *Arrows*, band positions of the genes being examined; the remaining band in each gel-panel is the β-actin internal control. In the upper and *lower panels*, the PCR products were resolved on 8% nondenaturing polyacrylamide gel. HD can be seen in sample 28 for both $p15^{INK4b}$ and $p16^{INK4a}$. In the middle two panels, the PCR products were resolved on 6% sequencing gel. HD of $p14^{ARF}$-E1β is apparent in samples 28 and 38. HD of $p16^{INK4a}$-E1α can be seen in sample 28 only. *P*, positive control using human placenta DNA.

confirmed that, indeed, only in the unmethylated-specific PCR product was every "C," including those in the CpG dinucleotide, changed to a "T" as a result of chemical modification. In the methylated-specific PCR product, the CpG sequence was not changed, indicating it is indeed amplified from DNA containing methylation (Fig. 3*b*).

Homozygous Deletion of the $p14^{ARF}$, $p15^{INK4b}$, and $p16^{INK4a}$ Genes. Gene deletion was examined by differential PCR analysis of the genomic DNA. Duplex PCR amplification was performed to generate a 177-bp fragment covering exon 1β of the $p14^{ARF}$ gene, a 172-bp fragment in the exon 2 of $p15^{INK4b}$, a 204-bp exon 1α fragment of $p16^{INK4a}$, or a 222-bp exon 2 fragment of $p16^{INK4a}$, together with a 187-bp fragment of the β-*actin* gene as a reference (Fig. 4). The β-actin fragment was amplified in all 40 pairs of normal and tumor samples. The $p14^{ARF}$-E1β product was amplified in all 40 normal samples, but it was either not detected or had a much lower intensity in 13 tumor samples (32.5%). We presumed that these 13 cases contained a homozygous deletion at the first exon of the $p14^{ARF}$ gene, and the low residue signals may come from wild-type stromal and infiltrative cells. Likewise, together with the previously analyzed paraffin samples, homozygous deletion of $p15^{INK4b}$ gene was observed in 16 (40%) of the 40 cases. In contrast, a relatively lower percentage of samples showed homozygous deletions of $p16^{INK4a}$. Seven of the 40 samples (17.5%) contained homozygous deletion at E2. We performed the homozygous deletion analysis for E1α on the 18 frozen samples (nos. 25–62) that had enough DNA for the study. Four of them showed homozygous deletion at E1α. The deletion pattern of E1α is the same as that of E2, suggesting that E2 was always codeleted with E1α because of their physical proximity. Only five cases contained homozygous deletion in all three loci, and 13 cases had deletion only at the centrameric end of the cluster (E1β-15^{INK4b} loci), whereas exclusive deletion of the $p16^{INK4a}$ at the telemeric end was observed in only two cases. In many cases, E1β of $p14^{ARF}$ was deleted together with $p15^{INK4b}$. However, two samples (nos. 38 and 920925) contained homozygous deletion at $p14^{ARF}$ only.

Mutational Analysis of E1β of the $p14^{ARF}$ Gene. Previously, we analyzed a collection of paraffin-embedded ESCC samples for $p16^{INK4a}$ gene mutation and detected no point mutation in the samples included in the present study (20). We further performed PCR-single strand conformation polymorphism analysis of E1β of the $p14^{ARF}$ gene in the 18 frozen ESCC samples, using methods described previously. We found no E1β mutation in these 18 samples, consistent with the reports from other laboratories (7).

Characterization of $p14^{ARF}$, $p15^{INK4b}$, and $p16^{INK4a}$ mRNA Expression. Levels of the $p14^{ARF}$, $p15^{INK4b}$, and $p16^{INK4a}$ transcripts were determined in 18 frozen ESCC samples by comparative RT-PCR analysis. A 264-bp fragment of the $p14^{ARF}$ gene transcript, a 428-bp fragment of the $p15^{INK4b}$ transcript, or a 176-bp fragment of the $p16^{INK4a}$ transcript were generated, respectively, with a 456-bp fragment of the GAPDH transcript coamplified as the internal standard. Although RT-PCR signals of the genes of interest were detected (at least with a minimal level) in almost all samples, nonparametric classification of the signal intensities (normalized by GAPDH signal) using the kNN method (22) revealed that the mRNA expression level of each of the genes had an apparent two-cluster distribution (Fig. 5). The two clusters correspond to minimally overlapped groups of data points and were therefore designated as class I and class II gene expression levels. Class I is tightly clustered with a small mean value and is well approximated by a Gaussian distribution. Class II has a significantly greater mean value and a much broader distribution not strictly Gaussian. Statistically, this suggests the presence of nonrandom regulating factors in samples showing class II mRNA levels but no such mechanisms underlining class I level mRNA expressions. On the average, the mRNA level of class II is ~10 times higher than that of class I. We interpret the two classes as representing distinctive states of gene expression; class I corresponds to a basal level, or suppressed state of gene expression, and class II corresponds to active gene expression. We defined the thresholds of suppressed and active $p14^{ARF}$, $p15^{INK4b}$, and $p16^{INK4a}$ gene expression as {[0, 0.26], [0.76, ∞]}, {[0, 0.15], [0.76, ∞]}, and {[0, 0.16], [0.50, ∞]}, respectively. The thresholds for the basal levels that correspond to the Gaussian-like class I were simply set to $\mu + 2\sigma$, whereas because of the spreadness of the distribution of class II, we take μ-σ as the lower limit of the active expression state to ensure enough separation between basal and active expression. Between the two thresholds is a

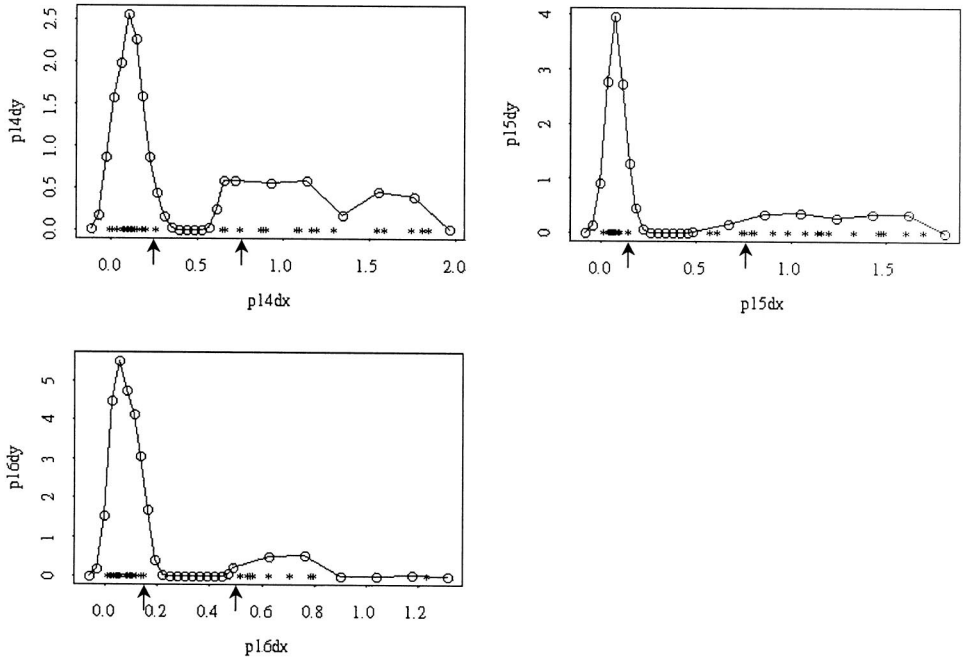

Fig. 5 Classification of the mRNA expression levels of the $p14^{ARF}$, $p15^{INK4b}$, and $p16^{INK4a}$ genes. Data points representing the measured expression signal intensities of each gene were classified by kNN classifier and were also analyzed using S-PLUS statistical software. The approximate probabilistic-distribution-density curve of the expression levels was plotted for each gene (*X axis*, expression level), and all of the values of the measured expression levels were marked by a * under the curve. It is apparent that the expression levels of each gene fall into two distinct classes. Arrow, thresholds for accepting a value as representing active or basal level expressions. Between the two thresholds is the rejection region, values that were considered as indeterminable in the case of expression state.

rejection region. Any mRNA level that fell into this range was considered as indeterminable of its expression state, or simply, as an intermediate state. From Fig. 6, It can be seen that chance occurrence to misclassify a value as indicating suppressed or active state is very low (strict calculation and mathematical discussion on this problem will appear in a separate report).

As summarized in Table 2, a great variation of gene expression exists in normal tissues adjacent to the ESCCs. Among all 18 normal samples, 9 and 7 actively expressed the $p14^{ARF}$ and $p15^{INK4b}$ genes, respectively, and for both genes an additional three showed intermediate level (close to the active threshold) expression, whereas basal level expressions of these two genes were less frequent. These seemed to suggest a frequent presence of oncogenic and extracellular growth factor stimuli in the cells close to cancer. However, although presumably also inducible by oncogenic stimuli (11), in most normal cases (14 of 18) the $p16^{INK4a}$ gene displayed only a basal level of expression. Taken together, there was no association in the expression of $p14^{ARF}$, $p15^{INK4b}$, and $p16^{INK4a}$ mRNA in the 18 normal samples, suggesting the existence of distinct regulations of each members of the 9p21 gene cluster.

Although the 456-bp GAPDH signal was invariant in all 18 ESCC tumor samples, suppressed mRNA expression was observed in 12 (67%) tumor samples for $p14^{ARF}$, in 9 (50%) tumor samples for $p15^{INK4b}$, and in 12 (67%) tumor samples for $p16^{INK4a}$ (Table 1 and Fig. 6). There is one tumor sample (no. 47) containing $p14^{ARF}$ expression at an intermediate level slightly above the threshold of suppression state. Detailed analyses revealed that for all three genes, the suppression of gene expression in tumors had two patterns. For example, among the 12 tumor cases that failed to actively express $p14^{ARF}$, 9 cases (nos. 25, 36, 38, 42, 43, 46, 47, 48, and 56) contained a high or intermediate level of $p14^{ARF}$ mRNA in the normal epithelia adjacent to the tumors (pattern I), and the remaining 4 cases (nos. 28, 33, 40, and 60) corresponded to a basal level of $p14^{ARF}$ expression in the accompanying normal epithelia (pattern II). Likewise, among the 9 tumor samples that showed suppressed $p15^{INK4b}$ expression, 5 were categorized as pattern I suppression, and 4 were categorized as pattern II suppression. Among the 12 tumor samples that showed suppressed $p16^{INK4a}$ expression, 3 showed pattern I suppression and 9 showed pattern II suppression. Taken together, only 4 of the 18 ESCC samples maintained an elevated level of mRNA expression for all of the three genes. The remaining 14 (77%) cases either showed suppression of all three genes (8 cases) or at least one of the three genes in the tumor (Fig. 7). These results suggested that the 9p21 gene cluster expression is frequently suppressed in ESCC cells.

Correlation Between Gene Expression and Molecular Alterations of the 9p21 Cluster. All promoter hypermethylation and homozygous deletion events detected in the $p14^{ARF}$, $p15^{INK4b}$, and $p16^{INK4a}$ genes corresponded to an absence or significant repression of the mRNA expression of the respective genes. Taken together, among the 12 frozen tumor samples showing repression of $p16^{INK4a}$ expression, 8 contained hypermethylation and 4 had deletions of the $p16^{INK4a}$ gene. Whereas among the nine samples with repressed $p15^{INK4b}$ expression, three had hypermethylation and six had homologous deletion. For $p14^{ARF}$, however, an exact correspondence of altered gene expression to alteration at E1β locus was not observed; among the 12 cases showing repressed expression, 2 had promoter hypermethylation, 6 had E1β deletion, and 4 had no detectable genetic alterations at the *E1*β locus. Sample 47, which had a close-to-suppression intermediate $p14^{ARF}$ expression, also harbored $p16^{INK4a}$ methylation.

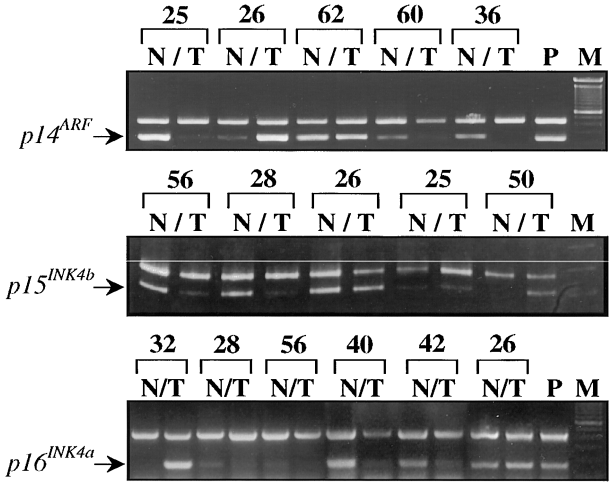

Fig. 6 mRNA expression pattern of *p14ARF*, *p15INK4b*, and *p16INK4a* genes. *Arrows*, band positions of the genes being examined; the remaining band in each gel panel is the GAPDH internal standard. RT-PCR products for *p15INK4b* analysis were resolved on 20% nondenaturing polyacrylamide gels, and products for *p14ARF* and *p16INK4a* were resolved on 3% agarose gels. *P*, positive control using human placenta RNA; *M*, 100-bp ladder marker. In the *upper panel*, samples 25, 60, and 36 display loss or very low level of *p14ARF* transcripts in the tumor. Among them, nos. 25 and 36 have a high level of gene transcripts in the matched normal tissues (pattern I), and no. 60 has a low level of gene transcripts in the normal tissue (pattern II). From the *middle panel*, samples 56 and 28 show pattern I repressed expression, and sample 25 has pattern II repressed expression in tumor. In the *lower panel*, samples 40 and 42 exhibit pattern I repressed expression, and samples 28 and 56 have pattern II repressed expression in tumor.

Discussion

The chromosome 9p21 region harbors three genes: *p14ARF*, *p15INK4b*, and *p16INK4a*, all of which have growth-suppressive activities. On the basis of the unusual genomic organization of this gene cluster and the functional relevance of these genes in both the Rb and p53 pathways, we reasoned that genes within this compact cluster can be differently regulated and are potentially susceptible to distinctive inactivating mechanisms, rather than a single deletion or methylation event occurring across the whole region. In the present study, we elucidated the mechanisms and approximate frequencies of aberrations affecting this subchromosomal region in human ESCCs and observed good correspondence between the molecular alteration and loss of gene expression.

Previous studies have demonstrated that the expression of *p14ARF*, *p15INK4b*, and *p16INK4a* normally undergo elevation in highly proliferative cells such as those affected by oncogenic stimuli (*e.g.*, H-rasV12 or SV40 T-antigen, which activate *p14ARF* and *p16INK4a*; Refs. 11 and 23), or growth factors (*e.g.*, TGF-β, which activates *p15INK4b*; Ref. 5) if the genes are intact. Upon activation, these gene products can counteract excessive cell proliferation. In our study, elevated levels of gene expressions were frequently observed for *p14ARF* and *p15INK4b*, and sometimes for *p16INK4a* in the morphologically normal epithelia adjacent to tumors, suggesting that abnormal growth stimuli might exist in these tissues. The $p14^{ARF}$, $p15^{INK4b}$ and $p16^{INK4a}$ possibly trigger an antiproliferation response there. The expression of *p14ARF*, *p15INK4b*, and *p16INK4a*, however, was frequently repressed in ESCC tumor samples; among which, 44% (8 of 18) of the samples showed repression of all three genes.

To date, two mechanisms have been postulated as primary causes of inactivation of the potential tumor suppressor genes on 9p21: homozygous deletion and promoter hypermethylation (24). *p16INK4a* has been widely regarded as the major target of 9p21 deletion. But because of the dual coding capacity of the *p16INK4a*-*p14ARF* locus, a deletion occurred on *p14ARF* exons 2 or 3 could still disrupt *p16INK4a*. There is evidence in a murine system that much of the tumorigenic phenotype associated with *p16INK4a* deletion may in fact be attributable to disruption of the *p14ARF* gene (23). However, whether *p14ARF* is a primary inactivation target is in debate. Point mutations in E1β are rare. Mutations in E2 of *p14ARF* and *p16INK4a* almost exclusively inactivate $p16^{INK4a}$ protein only (25). Deletion of *p14ARF* is either accompanied by deletion of *p15INK4b* or *p16INK4a* or both. Hypermethylation of *p14ARF* was observed in several colon cancer cell lines, which also contained hypermethylation on *p16INK4a* (7).

In our study, we found that deletion at the *p16INK4a* locus (7 of 40) was significantly less frequent than at *p14ARF* E1β and *p15INK4b* loci (13 of 40 and 16 of 40, respectively). In fact, most of the *p16INK4a* deletions (five of seven) only occurred in cases harboring complete 9p21 gene-cluster deletion. These results suggest that *p14ARF*, rather than the *p16INK4a* gene, is more likely to be a main target of deletion at 9p21. Although mostly deleted together with *p15INK4b*, possibly due to their physical proximity, *p14ARF*-specific deletion was seen in two ESCC samples (nos. 38 and 920925), and such event has also been reported previously (21, 26). Underlining the structural basis of this type of genomic changes, a recent study revealed the existence of tightly clustered breakpoints close to the *E1*α and *E1*β loci, and possibly also upstream of *p15INK4b* (21). There is evidence that the rearrangements in this region may involve illegitimate V(D)J recombinase activity, which could contribute to frequent gene-specific deletions (6). Recent studies suggested the importance of $p14^{ARF}$ as a potent tumor suppressor. Mice lacking *p19ARF* (the mouse homologue of *p14ARF*) develop a cancer phenotype (27), *p14ARF*-null embryonic fibroblasts, that exhibit a high rate of spontaneous immortalization and could be transformed by oncogenic *Ras* (23). The nature of *p14ARF* as a *bona fide* tumor suppressor gene in ESCC also owns to its remarkable frequency of transcriptional inactivation, 12 of 18 ESCCs, among the highest in the 9p21 gene cluster in our study. *p14ARF* can activate p53 both by neutralizing Mdm2, which destabilizes p53 (10), and by interacting directly with p53 (28) in response to oncogenic stimuli. Therefore, the loss of *p14ARF* function in tumor cells as observed in our study potentially compromises the p53-mediated cell cycle arrest and apoptotic process therein.

A second deletion hotspot is the *p15INK4b* locus. Although in most cases *p15INK4b* deletion was accompanied by a concomitant E1β deletion, 4 of the 16 deletion cases exclusively targeted *p15INK4b*. *p15INK4b* has often been considered as an innocent bystander of the deletion at 9p21 (24). Previous evidence of *p15INK4b* alteration in ESCC has been scarce, and its tumor suppressor role in esophageal carcinogenesis is uncertain. Our observation of frequent and sometimes elusive *p15INK4b* dele-

Table 2 Alterations of 9p21 gene cluster[a]

	p16^{INK4a}			*p14*^{ARF}			*p15*^{INK4b}		
	mRNA expression			mRNA expression			mRNA expression		
Sample no.	N	T	Gene alteration	N	T	Gene alteration	N	T	Gene alteration
25	0.04	0.04	m	1.55	0.08	m	0.05	0.06	m
26	0.57	0.71	+	0.19	1.59	+	0.76	1.17	+
28	0.09	0.02	−	0.00	0.00	−	0.75	0.06	−
32	0.03	1.24	+	0.05	1.81	+	0.10	0.99	+
33	0.08	0.10	m	0.15	0.16	+	0.07	0.02	m
36	0.15	0.14	m	0.88	0.00	+	1.20	1.08	+
38	0.10	0.52	+	1.10	0.11	−	0.10	0.81	+
40	0.80	0.15	m	0.09	0.09	+	1.70	1.61	+
42	0.55	0.06	−	0.75	0.02	−	0.02	0.15	−
43	0.09	0.06	m	1.30	0.13	−	1.48	0.06	−
46	0.10	0.04	m	0.75	0.13	−	0.80	0.08	−
47	0.11	0.05	m	0.90	0.27	+	0.15	1.49	+
48	0.15	0.04	−	1.85	0.19	+	1.33	0.99	+
50	0.05	0.56	+	1.08	0.65	+	0.08	0.91	+
53	0.63	0.80	+	1.17	1.75	+	1.14	1.45	+
56	0.04	0.01	m	0.67	0.10	m	0.62	0.05	m
60	0.12	0.09	−	0.21	0.10	−	0.05	0.10	−
62	0.03	0.80	+	1.20	0.90	+	0.58	0.08	−
4			m			m			+
6			−			+			+
704			−			−			−
705			+			m			−
91755			+			+			−
91779			+			−			−
91799			+			+			+
910657			−			−			−
910666			m			−			−
910673			m			−			−
910682			+			+			+
910793			m			m			m
910840			m			m			m
920925			m			−			+
920928			+			+			−
920934			+			+			+
920935			m			+			+
920943			+			+			−
920947			+			+			+
920950			m			−			−
920951			+			+			+
920973			+			+			+

[a] +, intact gene; −, homozygous deletion; m, methylation. For *p14*^{ARF}, − represents HD at E1β only.

tion suggests that *p15*^{INK4b} may itself be a tumor suppressor gene disrupted during ESCC development. Despite its close linkage and functional similarity to p16^{INK4a}, p15^{INK4b} plays a role of nonredundant cell cycle checkpoint. It is a mediator in the cell cycle control pathway originating from extracellular stimuli such as transforming growth factor β and IFN-α (5, 29). In principle, this pathway is independent of the intracellular pathway mediated by p16^{INK4a} and is equally crucial in maintaining a balanced cell cycle regulation. Tumorigenic transformation in somatic tissues are frequently preceded or accompanied by other cellular abnormalities, such as inflammation or increased proliferation. The growth factors secreted by the inflammatory cells and the increased cellular contact may produce such growth inhibition signal mediated by p15^{INK4b} to preclude cell cycle progression and therefore provide a way of counteracting the transformation tendency. It is possible that inactivation of *p15*^{INK4b} can desensitize the cell to such extracellular signals and as a result contribute to cancer development. Indeed, evidence of specific inactivation of the *p15*^{INK4b} gene has been increasing in recent studies in acute lymphoblastic leukemia (30) and other solid tumors (summarized in Ref. 2).

Our observation of relatively infrequent homozygous deletion at the *p16*^{INK4a} locus is consistent with most previous studies on primary ESCC tumors (31, 32) but disagrees with the results from ESCC cell lines (summarized in Ref. 33). Hayashi *et al.* (34) suggested that simultaneous loss of *p16*^{INK4a} and *p14*^{ARF} expression, which was observed in 11 of 18 frozen tumor samples in our study, is an indicator of homozygous deletion of *p16*^{INK4a}. However, we found that 8 of the 11 cases actually contained hypermethylation on the *p16*^{INK4a} promoter. Most of the methylation took place exclusively on the *p16*^{INK4a} promoter. On the basis of the significantly higher frequency (40%) of hypermethylation on *p16*^{INK4a} compared with *p14*^{ARF} (15%) and *p15*^{INK4b} (12.5%), and its relatively low deletion rate,

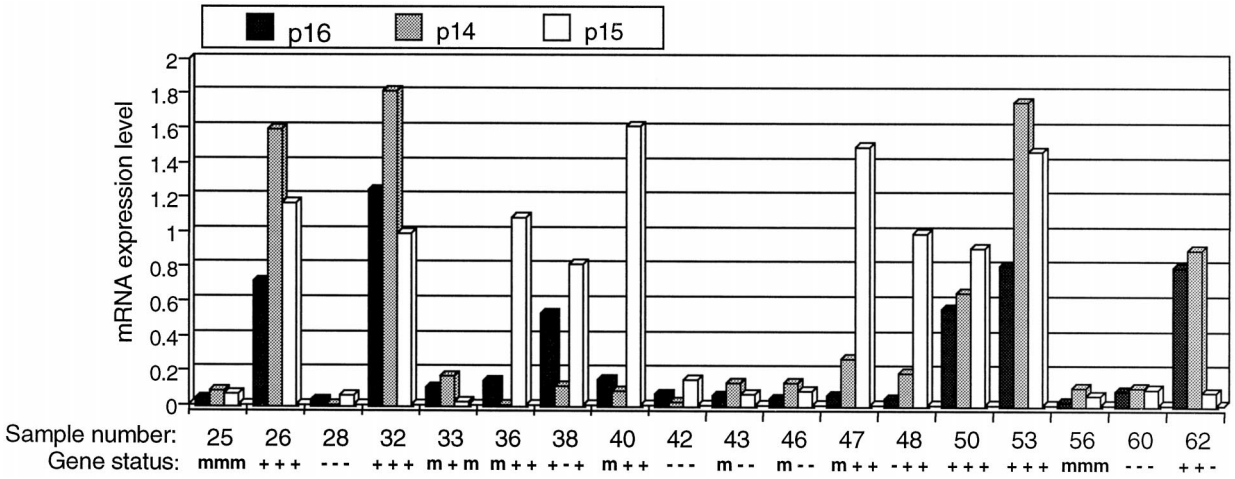

Fig. 7 Summary of mRNA expression pattern of $p14^{ARF}$, $p15^{INK4b}$, and $p16^{INK4a}$ genes and their corresponding molecular status in 18 frozen ESCC samples. As shown in the histogram, only 4 of the 18 samples (nos. 26, 32, 50, and 53) maintain active expression of all three genes in tumor, whereas 8 cases have low expression of all three genes in tumor.

we propose that $p16^{INK4a}$ is a primary target of aberrant hypermethylation in ESCC. Our hypothesis of $p16^{INK4a}$ as a primary methylation target can easily explain observations in the previous report of cases that fail to express $p16^{INK4a}$ but express $p14^{ARF}$ readily (34), because $p14^{ARF}$ is controlled by a different promoter (3), which may not be comethylated with $p16^{INK4a}$. The preferential methylation of the $p16^{INK4a}$ promoter may relate to its special local genomic structure, featured by a cluster of breakpoints located just 5′ to E1α, the sequence content of which bears the hallmark of V(D)J recombinase activity (6). It was shown that aberrant DNA structures, such as integration intermediates, seem to unleash *de novo* activity of the mammalian DNA methyltransferase (35). In our study, the sharp difference of deletion rates between the $p16^{INK4a}$ and E1β-$p15^{INK4b}$ loci suggests possible rearrangement hotspot upstream of the $p16^{INK4a}$ locus. Therefore, frequent $p16^{INK4a}$ promoter methylation may be relevant to the frequent rearrangement events upstream of $p16^{INK4a}$. Transcriptional silencing promoter-methylation has been rarely observed for $p14^{ARF}$ and $p15^{INK4b}$ in epithelium-derived tumors. Our observation of both events revealed an alternative mode of $p14^{ARF}$ and $p15^{INK4b}$ inactivation in ESCCs, although at a low frequency. Except for one case with methylation exclusively on $p14^{ARF}$, all methylation events beyond the $p16^{INK4a}$ gene have concomitant $p16^{INK4a}$ methylation, suggesting they have an association with $p16^{INK4a}$ methylation and can also be exclusively targeted.

Although all abnormalities of $p16^{INK4a}$ and $p15^{INK4b}$ expression correspond to an underlining homozygous deletion or hypermethylation of the gene, we were unable to establish a good match between the E1β alterations and inactive $p14^{ARF}$ expression. Specifically, we observed four tumors samples that showed inactive $p14^{ARF}$ expression but contained neither detectable E1β deletion or promoter methylation. Among them, one case (no. 48) can be easily explained by a deletion at $p16^{INK4a}$ because that event also removed part of the $p14^{ARF}$ gene sequence shared with $p16^{INK4a}$. The remaining three cases (nos. 33, 36, and 40), together with a sample (no. 47) with lower intermediate level of $p14^{ARF}$ expression, all appeared to have intact $p14^{ARF}$ gene, except that they all contained hypermethylation in the downstream $p16^{INK4a}$ locus. Gonzalgo *et al.* (36) have shown in cell lines that hypermethylation of $p16^{INK4a}$ had no effect on the transcription of $p14^{ARF}$. It would be very interesting to determine whether other factors, such as p53, which is stabilized by $p14^{ARF}$ and causes the down-regulation of $p14^{ARF}$ (7), also contribute to $p14^{ARF}$ inactivation.

In summary, our results show that the newly identified growth suppressor $p14^{ARF}$, together with $p15^{INK4b}$, is a primary target of homozygous deletion, whereas $p16^{INK4a}$ is the hypermethylation hotspot in human ESCC. Such a polarity may reflect the presence of sequence-specific elements that favor such alteration or the effect of growth selection during cancer formation. Because recent studies have shown that oncogenic stimuli elicit the antitumorigenic response by up-regulating both $p14^{ARF}$ and $p16^{INK4a}$, which in turn activate the tumor suppressors p53 and pRb, respectively (10, 11), the tumor suppressor role of the 9p21 gene cluster becomes apparent. The unique genomic structure and compact organization of these genes as a cluster may be essential for the highly coordinated regulation in maintaining a balanced Rb and p53 pathway function. Our observation of frequent coinactivation of $p14^{ARF}$ and $p16^{INK4a}$, and even inactivation of the entire 9p21 gene cluster, provides additional evidence for the dysfunction of both Rb and p53 tumor suppression pathways in ESCC development.

Acknowledgments

We thank Jinshang Zhang of the Department of Statistics at Rutgers University for help in the statistical analysis of our data and in generating the density distribution plots on his workstation. We also thank Dr. Jie Liao for assistance in preparing the frozen tissue samples for our analysis.

References

1. Sherr, C. J. Cancer cell cycles. Science (Washington DC), *274:* 1672–1677, 1996.

2. Carnero, A., and Hannon, G. J. The INK4 family of CDK inhibitors. Curr. Top. Microbiol. Immunol., *227:* 43–55, 1998.

3. Stone, S., Jiang, P., Dayananth, P., Tavtigian, S. V., Katcher, H., Parry, D., Peters, G., and Kamb, A. Complex structure and regulation of the *P16* (*MTS1*) locus. Cancer Res., *55:* 2988–2994, 1995.

4. Quelle, D. E., Zindy, F., Ashmun, R. A., and Sherr, C. J. Alternative reading frames of the *INK4a* tumor suppressor gene encode two unrelated proteins capable of inducing cell cycle arrest. Cell, *83:* 993–1000, 1995.

5. Hannon, G. J., and Beach, D. p15INK4B is a potential effector of TGF-β-induced cell cycle arrest [see comments]. Nature (Lond.), *371:* 257–261, 1994.

6. Cayuela, J. M., Gardie, B., and Sigaux, F. Disruption of the multiple tumor suppressor gene *MTS1/p16(INK4a)/CDKN2* by illegitimate V(D)J recombinase activity in T-cell acute lymphoblastic leukemias. Blood, *90:* 3720–3726, 1997.

7. Robertson, K. D., and Jones, P. A. The human ARF cell cycle regulatory gene promoter is a CpG island which can be silenced by DNA methylation and down-regulated by wild-type p53. Mol. Cell. Biol., *18:* 6457–6473, 1998.

8. Chin, L., Pomerantz, J., and DePinho, R. A. The *INK4a/ARF* tumor suppressor: one gene–two products–two pathways. Trends Biochem. Sci., *23:* 291–296, 1998.

9. Serrano, M., Hannon, G. J., and Beach, D. A new regulatory motif in cell-cycle control causing specific inhibition of cyclin D/CDK4 [see comments]. Nature (Lond.), *366:* 704–777, 1993.

10. Pomerantz, J., Schreiber-Agus, N., Liegeois, N. J., Silverman, A., Alland, L., Chin, L., Potes, J., Chen, K., Orlow, I., Lee, H. W., Cordon-Cardo, C., and DePinho, R. A. The Ink4a tumor suppressor gene product, p19Arf, interacts with MDM2 and neutralizes MDM2's inhibition of p53. Cell, *92:* 713–723, 1998.

11. Serrano, M., Lin, A. W., McCurrach, M. E., Beach, D., and Lowe, S. W. Oncogenic *ras* provokes premature cell senescence associated with accumulation of p53 and p16INK4a. Cell, *88:* 593–602, 1997.

12. Palmero, I., Pantoja, C., and Serrano, M. p19ARF links the tumour suppressor p53 to Ras. Nature (Lond.), *395:* 125–126, 1998.

13. Bates, S., Phillips, A. C., Clark, P. A., Stott, F., Peters, G., Ludwig, R. L., and Vousden, K. H. p14ARF links the tumour suppressors RB and p53. Nature (Lond.), *395:* 124–125, 1998.

14. Hirama, T., and Koeffler, H. P. Role of the cyclin-dependent kinase inhibitors in the development of cancer. Blood, *86:* 841–854, 1995.

15. Orlow, I., Lacombe, L., Hannon, G. J., Serrano, M., Pellicer, I., Dalbagni, G., Reuter, V. E., Zhang, Z. F., Beach, D., and Cordon-Cardo, C. Deletion of the *p16* and *p15* genes in human bladder tumors [see comments]. J. Natl. Cancer Inst., *87:* 1524–1529, 1995.

16. Cairns, P., Polascik, T. J., Eby, Y., Tokino, K., Califano, J., Merlo, A., Mao, L., Herath, J., Jenkins, R., Westra, W., Rutter, L., Buckler, A., Gabrielson, E., Tockman, M., Cho, K. R., Hedrick, L., Bova, G. S., Issacs, W., Koch, W., Schwab, D., and Sidransky, D. Frequency of homozygous deletion at p16/CDKN2 in primary human tumours. Nat. Genet., *11:* 210–212, 1995.

17. Herman, J. G., Merlo, A., Mao, L., Lapidus, R. G., Issa, J. P., Davidson, N. E., Sidransky, D., and Baylin, S. B. Inactivation of the *CDKN2/p16/MTS1* gene is frequently associated with aberrant DNA methylation in all common human cancers. Cancer Res., *55:* 4525–4530, 1995.

18. Herman, J. G., Civin, C. I., Issa, J. P., Collector, M. I., Sharkis, S. J., and Baylin, S. B. Distinct patterns of inactivation of p15INK4B and p16INK4A characterize the major types of hematological malignancies. Cancer Res., *57:* 837–841, 1997.

19. Pollock, P. M., Pearson, J. V., and Hayward, N. K. Compilation of somatic mutations of the *CDKN2* gene in human cancers: non-random distribution of base substitutions. Genes Chromosomes Cancer, *15:* 77–88, 1996.

20. Xing, E. P., Nie, Y., Wang, L. D., Yang, G. Y., and Yang, C. S. Aberrant methylation of $p16^{INK4a}$ and deletion of $p15^{INK4b}$ are frequent events in human esophageal cancer in Linxian, China. Carcinogenesis, *20:* 77–84, 1999.

21. Gardie, B., Cayuela, J. M., Martini, S., and Sigaux, F. Genomic alterations of the p19ARF encoding exons in T-cell acute lymphoblastic leukemia. Blood, *91:* 1016–1020, 1998.

22. Fukunaga, K. Statistical Pattern Recognition, Ed. 2. San Diego, CA: Academic Press, Inc., 1990.

23. Kamijo, T., Zindy, F., Roussel, M. F., Quelle, D. E., Downing, J. R., Ashmun, R. A., Grosveld, G., and Sherr, C. J. Tumor suppression at the mouse *INK4a* locus mediated by the alternative reading frame product p19ARF. Cell, *91:* 649–659, 1997.

24. Kamb, A. Cyclin-dependent kinase inhibitors and human cancer. Curr. Top. Microbiol. Immunol., *227:* 139–148, 1998.

25. Quelle, D. E., Cheng, M., Ashmun, R. A., and Sherr, C. J. Cancer-associated mutations at the *INK4a* locus cancel cell cycle arrest by p16INK4a but not by the alternative reading frame protein p19ARF. Proc. Natl. Acad. Sci. USA, *94:* 669–673, 1997.

26. Larsen, C. J. *p16INK4a*: a gene with a dual capacity to encode unrelated proteins that inhibit cell cycle progression. Oncogene, *12:* 2041–2044, 1996.

27. Serrano, M., Lee, H., Chin, L., Cordon-Cardo, C., Beach, D., and DePinho, R. A. Role of the *INK4a* locus in tumor suppression and cell mortality. Cell, *85:* 27–37, 1996.

28. Kamijo, T., Weber, J. D., Zambetti, G., Zindy, F., Roussel, M. F., and Sherr, C. J. Functional and physical interactions of the ARF tumor suppressor with p53 and Mdm2. Proc. Natl. Acad. Sci. USA, *95:* 8292–8297, 1998.

29. Sangfelt, O., Erickson, S., Einhorn, S., and Grander, D. Induction of Cip/Kip and Ink4 cyclin dependent kinase inhibitors by interferon-α in hematopoietic cell lines. Oncogene, *14:* 415–423, 1997.

30. Iravani, M., Dhat, R., and Price, C. M. Methylation of the multi tumor suppressor gene-2 (*MTS2*, *CDKN1*, *p15INK4B*) in childhood acute lymphoblastic leukemia. Oncogene, *15:* 2609–2614, 1997.

31. Igaki, H., Sasaki, H., Tachimori, Y., Kato, H., Watanabe, H., Kimura, T., Harada, Y., Sugimura, T., and Terada, M. Mutation frequency of the *p16/CDKN2* gene in primary cancers in the upper digestive tract. Cancer Res., *55:* 3421–3423, 1995.

32. Maesawa, C., Tamura, G., Nishizuka, S., Ogasawara, S., Ishida, K., Terashima, M., Sakata, K., Sato, N., Saito, K., and Satodate, R. Inactivation of the *CDKN2* gene by homozygous deletion and *de novo* methylation is associated with advanced stage esophageal squamous cell carcinoma. Cancer Res., *56:* 3875–3878, 1996.

33. Chan, W. C., Tang, C. M., Lau, K. W., and Lung, M. L. *p16* tumor suppressor gene mutations in Chinese esophageal carcinomas in Hong Kong. Cancer Lett., *115:* 201–206, 1997.

34. Hayashi, K., Metzger, R., Salonga, D., Danenberg, K., Leichman, L. P., Fink, U., Sendler, A., Kelsen, D., Schwartz, G. K., Groshen, S., Lenz, H. J., and Danenberg, P. V. High frequency of simultaneous loss of *p16* and *p16*β gene expression in squamous cell carcinoma of the esophagus but not in adenocarcinoma of the esophagus or stomach. Oncogene, *15:* 1481–1488, 1997.

35. Laird, P. W., and Jaenisch, R. The role of DNA methylation in cancer genetic and epigenetics. Annu. Rev. Genet., *30:* 441–464, 1996.

36. Gonzalgo, M. L., Hayashida, T., Bender, C. M., Pao, M. M., Tsai, Y. C., Gonzales, F. A., Nguyen, H. D., Nguyen, T. T., and Jones, P. A. The role of DNA methylation in expression of the *p19/p16* locus in human bladder cancer cell lines. Cancer Res., *58:* 1245–1252, 1998.